Electro-thermal characterization of a differential temperature sensor in a 65 nm CMOS IC: Applications to gain monitoring in RF amplifiers

Josep Altet, José Luis Gonzalez, Didac Gomez, Xavier Perpiñà, Wilfrid Claeys, Stéphane Grauby, Cedric Dufis, Miquel Vellvehi, Diego Mateo, Ferran Reverter, et al.

Electro-thermal characterization of a differential temperature sensor in a 65 nm CMOS IC: Applications to gain monitoring in RF amplifiers

Josep Altet [a,*], José Luis González [c], Dídac Gomez [a,1], Xavier Perpiñà [b], Wilfrid Claeys [d], Stephane Grauby [d], Cedric Dufis [a], Miquel Vellvehi [b], Diego Mateo [a], Ferran Reverter [a], Stefan Dilhaire [d], Xavier Jordà [b]

[a] Electronic Engineering Department, Universitat Politècnica de Catalunya, Spain
[b] IMB-CNM (CSIC), Bellaterra – Spain
[c] CEA-Leti, Minatec Campus, Grenoble, France
[d] Laboratoire Ondes et Matière d'Aquitaine, Université Bordeaux I, France

Keywords:
CMOS integrated circuits
CMOS differential temperature sensors
Electro-thermal characterization
Thermal coupling characterization
IR camera measurements
Laser interferometer measurements

A B S T R A C T

This paper reports on the design solutions and the different measurements we have done in order to characterize the thermal coupling and the performance of differential temperature sensors embedded in an integrated circuit implemented in a 65 nm CMOS technology. The on-chip temperature increases have been generated using diode-connected MOS transistors behaving as heat sources. Temperature measurements performed with the embedded sensor are corroborated with an infra-red camera and a laser interferometer used as thermometer. A 2 GHz linear power amplifier (PA) is as well embedded in the same silicon die. In this paper we show that temperature measurements performed with the embedded temperature sensor can be used to monitor the PA DC behavior and RF activity.

1. Introduction

Nowadays integrated circuits and system-on-chip (SoC) designs are embedded with several sensors in order to monitor relevant physical and electrical magnitudes. The information provided by the on-chip sensor have several applications: reliability enhancement (e.g. absolute temperature monitoring [1]), structural integrity verification (i.e. built-in-test approaches [2]), variability monitoring [3], and yield enhancement (so called self-healing strategies [4]). If the sensor is used to monitor the performances or the structural integrity of high frequency analog circuits, one of the requirements is that it should be non-intrusive, i.e. it should not electrically load any node of the circuit under measurement. The contact to the RF circuitry should be avoided for two reasons: firstly, this avoids the need of co-designing simultaneously the sensor and the circuit under measurement; secondly, this prevents the input impedance of the sensor from affecting the performances of the circuit under measurement. One of the non-intrusive solutions proposed in the literature is the use of temperature sensors to extract figures of merit of high frequency analog circuits. The principle is simple: the operation of analog circuit relies on electrical signals, which cause power to be dissipated by the circuit devices, which in its turn causes a temperature increase in the semiconductor die. Therefore, the sensed temperature variations may depend on the circuit operation. For instance [5], presents the characterization of the central frequency and 1 dB compression point of a 1 GHz low noise amplifier from low frequency temperature measurements. In [6], the gain of a 2 GHz class A linear power amplifier is monitored with DC temperature measurements.

The understanding of the correlation between the temperature measurements and the figures-of-merit (FoM) of the high frequency analog circuit requires an accurate thermal coupling characterization between the circuit under measure and the temperature sensor placed close to it, as well as a good characterization of the temperature sensor that is used to perform the measurements.

The aim of this paper is to show the design decisions and the characterization of the thermal coupling that exists between differential temperature sensors used to monitor high frequency analog blocks and devices/circuits embedded in the same silicon

* Corresponding author. Tel: +34 934017481; fax: + 34 934016756.
E-mail address: josep.altet@upc.edu (J. Altet).
[1] D. Gómez is currently with Broadcom.

die. The integrated circuit (IC) we use in this paper to perform the measurements is the same that has been used in [6].

The paper is structured as follows: in Section 2 we review the principle of temperature measurement for test/characterization purposes and define the figures of merit that characterize the thermal coupling. The section describes as well the integrated circuit that is going to be characterized in this paper. Section 3 presents a detailed characterization of the temperature sensor itself when temperature increases have been generated with single MOS transistors placed in strategic places of the IC whose power dissipation can be externally controllable. Section 3.4 shows the thermal coupling that exists between a 2 GHz PA and the temperature sensor embedded in the same silicon die, demonstrating that with DC temperature measurements it is possible to track both the DC bias of the PA and its RF activity. Temperature measurements performed with the embedded sensor are corroborated with other off-chip temperature sensing strategies: an IR camera and a laser interferometer used as thermometer. Finally, Section 4 concludes the paper.

2. Principle of thermal testing of analog circuits. Integrated circuit description

2.1. Principle of thermal testing

To make the paper self-contained and to present the variables that are going to be characterized in the experimental measurements, this section briefly resumes the principle of thermal testing of analog circuits. Detailed examples can be found in [4–6]. Fig. 1 represents an integrated circuit with a circuit under test (CUT) and a differential temperature sensor. The differential temperature sensor has two temperature transducers whose temperatures are, respectively, T_1 and T_2.

The CUT can be any generic analog bloc, e.g. a low noise amplifier, a power amplifier, etc. Several CUT may be present in the same IC that can be sequentially activated to perform thermal measurements.

The temperature sensor is differential, i.e., it verifies

$$\Delta V_{OUT} = S_{Td}(T_2 - T_1) \tag{1}$$

where S_{Td} is sensor's thermal differential sensitivity (V/°C) [8].

If we assume that prior the CUT activation the silicon surface is at the ambient temperature T_a, then, when the CUT is activated

$$\begin{aligned} T_1 &= T_a + \Delta T_1 \\ T_2 &= T_a + \Delta T_2 \end{aligned} \tag{2}$$

where ΔT_1 and ΔT_2 are the temperature increases at the temperature transducers locations due to CUT activity. The sensor output becomes

$$\Delta V_{OUT} = S_{Td}(\Delta T_2 - \Delta T_1). \tag{3}$$

For simplicity, let us consider the case where the CUT only has DC power dissipation. Then the temperature increase is DC

$$\begin{aligned} \Delta T_1 &= R_{TH1} P_{CUT} \\ \Delta T_2 &= R_{TH2} P_{CUT} \\ \Delta V_{OUT} &= S_{Td}(\Delta T_2 - \Delta T_1) = S_{Td}(R_{TH2} - R_{TH1}) P_{CUT} \\ &= S_{Td} \Delta R_{TH} P_{CUT} = S_{Pd} P_{CUT} \end{aligned} \tag{4}$$

where P_{CUT} is the power dissipated by the CUT, R_{THi} is the thermal coupling resistance between the CUT and the temperature transducer (°C/W) i and S_{Pd} is the differential sensitivity to the power dissipated by the CUT (V/W). It is interesting to highlight that although S_{Td} only depends on the temperature sensor topology, S_{Pd} depends as well on the placement of the temperature transducers with respect to the active CUT location in the layout and it might become negative.

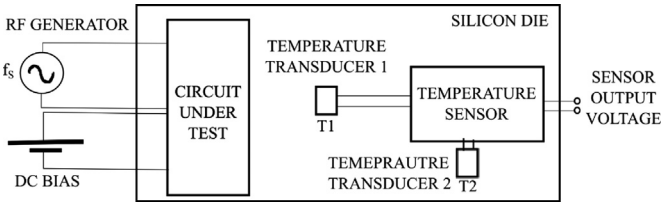

Fig. 1. Schematic of an integrated circuit that contains a generic circuit under test and a differential temperature sensor.

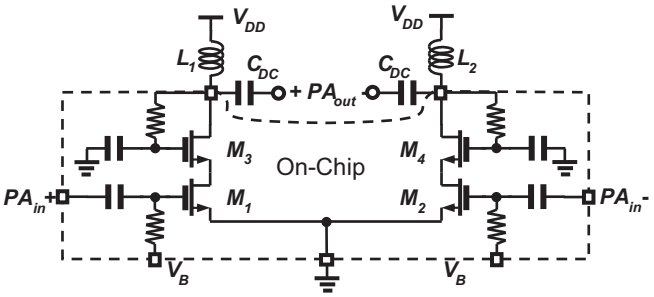

Fig. 2. Simplified schematic of a linear class A power amplifier.

The goal of the thermal testing is to observe the CUT performances from its dissipated power. For instance, the work [6] shows how the DC power dissipated by a 2 GHz class A power amplifier (the same that is going to be used in this paper) depends on the amplifiers gain. Therefore, the power amplifier (PA) gain can be monitored by temperature measurements.

In this paper, we characterize the differential sensitivity (i.e. the thermal coupling to temperature sensors) to the power dissipated by several CUTs: the 2 GHz PA and some MOS devices used as controllable dissipating elements. Moreover, we discuss how the placement and the frequency affect the value of the differential sensitivity.

2.2. Integrated circuit description

In this section we describe the schematic and the placement of the different CUTs and the temperature sensors embedded in the IC used for the experiments described in this paper.

Fig. 2 shows the schematic of the PA designed for a 2 GHz transmitter for coax-cable communications. It has been implemented using a 65 nm CMOS process. It is based in a pseudo-differential common-source cascode amplifier. The inductors L_1 and L_2, as well as the C_{DC} capacitors, are off-chip components and are used to center the PA in one of four possible sub-bands of the coax-cable standard, particularly the one between 2 and 2.5 GHz. More details about this circuit can be found in [7]. The main characteristics of such PA have been experimentally obtained: power gain @ 2.3 GHz = 17.8 dB, P_{DC} = 96 mW (@V_{DD} = 1.1 V), and OCP1 = 10.5 dBm.

Fig. 3 shows the schematic of the differential temperature sensor. This sensor is based on the circuit published in [8]. The two temperature transducers are the bipolar transistors Q_1 and Q_2, whose temperatures are T_1 and T_2, respectively. As indicated in (1), the output voltage of this sensor can be written as

$$V_{OUT} = S_{Td}(T_1 - T_2) + V_{offset}, \tag{5}$$

where V_{offset} is the sensor output voltage when there is no thermal imbalance between the two temperature transducers. In this design, the temperature transducers are vertical NPN bipolar transistors built using the deep-nwell/pwell/n+diffusion structure available in the

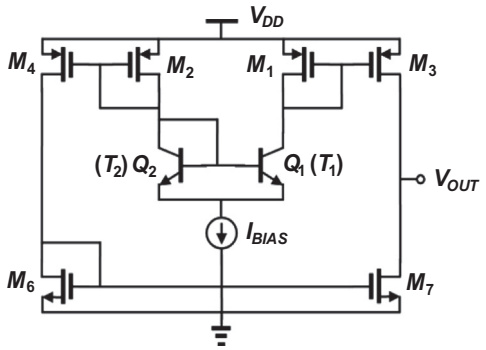

Fig. 3. Schematic of the differential temperature sensor embedded in the same IC than the power amplifier.

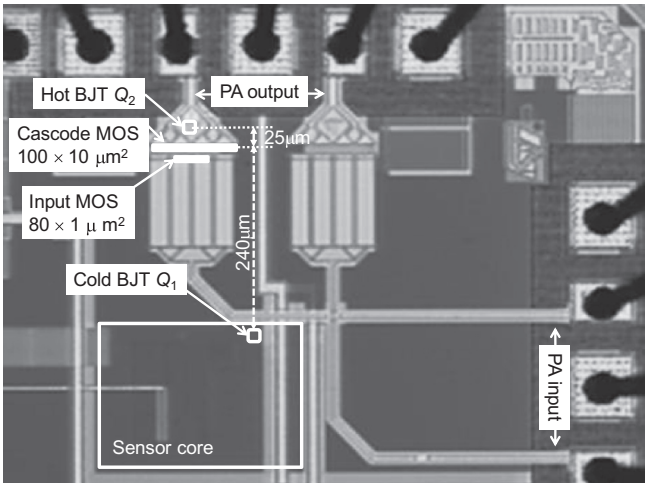

Fig. 4. Placement of the sensor and the PA devices within the integrated circuit layout.

selected CMOS process. The working principle is as follows: when the temperature transducers operate at different temperature, the differential pair collector current is unbalanced from the equilibrium state. The current mirrors M1–M3, M2–M4 and M6–M7 bring this current imbalance to the output branch, where the high impedance of the output stage converts it into changes of the output voltage V_{OUT}. A detailed analysis can be found in [8]. To avoid self-heating, the power consumption of the sensor is low: P_{DC}=800 μW (@V_{DD}=1.2 V).

Fig. 4 shows the placement of the temperature sensor and the PA devices in the IC surface. The goal of this placement is to ensure that the two temperature transducers have a different temperature increase when the PA dissipates power (the term ΔR_{TH} in (4) is different from zero). To this end, the temperature transducer Q_2 is placed close to the power amplifier (at 25 μm from transistors M_3 in Fig. 1). The temperature transducer Q_1 is placed at 240 μm far from Q_2, together with the other devices that form the temperature sensor. As thermal coupling from the PA affects more Q_2 than Q_1, the former is called hot transistor, whereas we named the latter cold transistor. The hot transistor is placed closer to the cascode transistor (M_3 in Fig. 2) than to the input transistor (M_1 in Fig. 2) because the former experiences higher RF amplitude swing in its drain to source voltage, thus having a DC power dissipation with stronger correlation to the RF PA behavior [5]. The short distance between the PA transistors and Q_2 ensures that the thermal settling time is smaller than 100 μs. Q_1 and the sensor core devices have been placed in empty space available in a previously existing layout of the IC, so they have not supposed

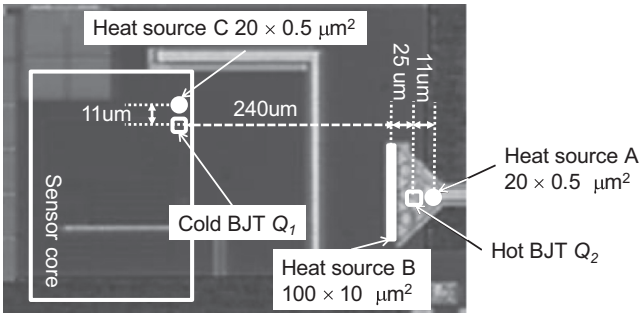

Fig. 5. Detail of the placement of the temperature sensor used for the thermal coupling characterization and the three devices acting as heat sources.

any area penalty to the IC. Similarly, the hot temperature transducer is placed in a very small area that was available in the layout. The sensor has been added to a previously designed IC without any area impact or resizing. Just some additional routing has been required in order to connect the hot transducer to the sensor core and the sensor output to an additional pad.

To perform a detailed thermal coupling and sensor characterization, we have placed in the same silicon die another identical differential temperature sensor (with the same dimensions, device placement and distance between hot and cold transducers) jointly with three MOS transistors whose dissipated power can be controlled (they are connected in diode configuration, i.e. with their gate tied to the drain and connected to an external pin, whereas their source is tied to ground). For this reason, these transistors are named heat sources. They are used to monitor how the sensor reacts as a function of their dissipated power (they are used as very simple CUT). Two of the transistors are sized W/L=20 μm/0.5 μm. The first, named heat source A in Fig. 5, is placed at 11 μm from the hot transducer, whereas the second, called heat source C in Fig. 5, at 11 μm from the cold transducer. The third transistor, called heat source B in Fig. 5, has been placed at 25 μm from the hot temperature transducer. The latter has the same dimensions than the PA cascode transistor (W/L=100 μm/10 μm, M_3 in Fig. 2) and the distance between the hot transducer and this transistor is the same than the existing between the PA cascode transistor and the hot transducer of the temperature sensor placed close to it. The purpose of these transistor dimensions and layout placement is to measure the thermal coupling that must exist between the transistor M_3 of the PA and the hot temperature transducer.

3. Temperature sensor characterization

3.1. Characterization of the differential sensitivity. DC measurements

When a CUT dissipates power, it generates a thermal gradient in the silicon surface that affects in a different way the two temperature transducers. Combining Eqs. (4) and (5)

$$V_{OUT} = S_{Pd} P_{CUT} + V_{offset}. \tag{6}$$

As we will see along this section, S_{Pd} depends on the nature of the CUT, its placement and the temperature sensor placement. This subsection aims at measuring S_{Pd} for each heat source. We are going to present measurements obtained in two different samples. Fig. 6 shows the sensor output voltage evolution as a function of the power dissipated by each heat source when the other two are off (the sensor power supply is set to V_{DD}=1.2 V). The sensor output voltage variations that appear when either the heat source A or C is activated shows the symmetrical behavior of the sensor expressed by Eq. (5): when the heat source A is active, the hot

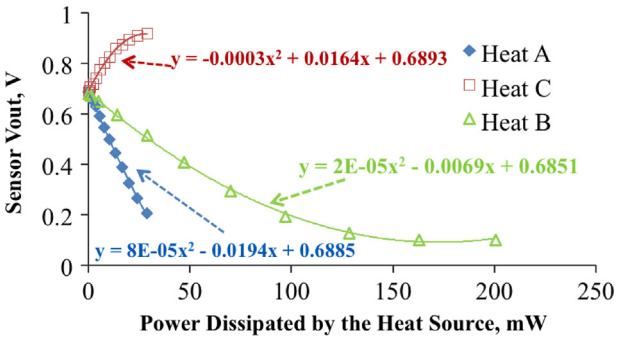

Fig. 6. Sensor output voltage as a function of the power dissipated by each heat source (the other two are off). V_{DD}=1.2 V. Sample 1.

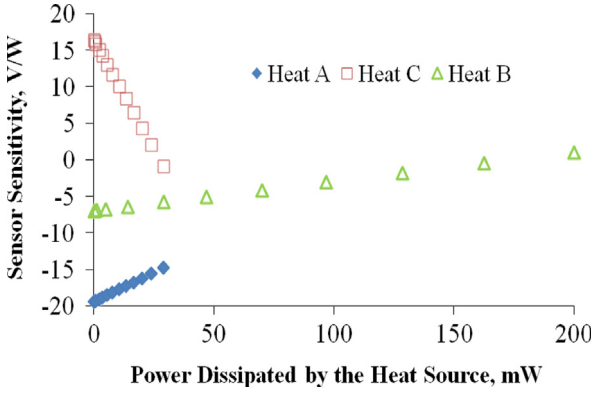

Fig. 7. Sensor differential sensitivity (V/W) as a function of the DC power dissipated by each heat source. Sample 1.

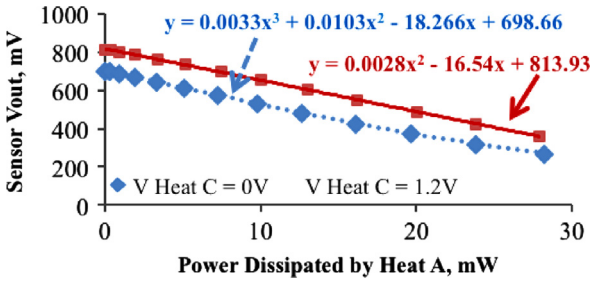

Fig. 8. Sensor output voltage as a function of the power dissipated by heat source A. Two values of power dissipation by heat source C: 0 W and 12.48 mW. V_{DD}=1.2 V. Sample 2.

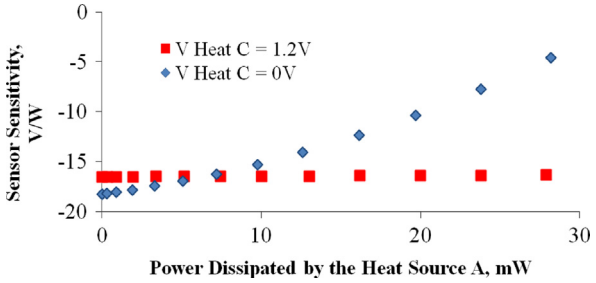

Fig. 9. Sensor differential sensitivity (V/W) as a function of the DC power dissipated by the heat source A. Sample 2.

transducer increases its temperature proportionally to the power dissipated by the heat source A (i.e. (T_1-T_2) in Eq. (5) becomes negative) and the sensor output voltage decreases. On the other hand, when the heat source C is active, the cold transducer increases its temperature (i.e. (T_1-T_2) in Eq. (5) becomes positive) and the sensor output voltage increases. As these two heat sources are identical in size and placed at the same distance from each temperature transducer, they are expected to induce a similar temperature increase to the closest temperature transducer when they dissipate the same amount of power. Another interesting result comes when comparing the measurements obtained with heat sources A and B: due to the different dissipated power density (MOS transistors A and B have different gate area – see Fig. 5) and to the different distance between the heat source and the transducer, for the same amount of dissipated power, the heat source A induces a higher temperature increase in the hot temperature transducer than the heat source B.

The differential sensitivity of the sensor to the power dissipated by each heat source can be found from the derivative of the functions reported in Fig. 6. To this end, these plots have been fitted with a second order polynomial function. Fig. 7 shows the sensitivities (expressed in V/W) of the sensor output voltage as a function of the power dissipated by each heat source. There are some interesting points to analyze from these results. Firstly, as expected from Eqs. (4–6), the sensitivity associated to the heat source A is negative, whereas the one associated to the heat source C is positive. However, from Eq. (4), we would expect an identical sensitivity in absolute value, which is not the case. This can be attributed to several reasons. The first one is the sensor topology itself: the differential sensitivity depends linearly on the sensor output resistance [8], which has a strong dependence on the operating point of the two output MOS transistors: M_3 and M_7 in Fig. 2. In addition to this, heat source C also modifies the temperature of the sensor core devices, as it is placed very close to them. Moreover, the base current of both bipolar devices depends on temperature, which introduces an additional source of unbalance in sensor's differential pair, as all base currents come from only one of the sensor differential branches. It has to be also considered that when the output voltage is close to any of the supply rails, the sensor enters into saturation and sensitivity nulls. Finally, as indicated in Eq. (5), the differential sensitivity to the dissipated power depends on the thermal coupling resistance. Different boundary conditions and different layout (e.g. the number of metal contacts) can make the thermal coupling resistance between the heat source A or C and its closest temperature transducer differ one from the other.

When two heat sources are simultaneously activated, V_{offset}, S_{Pd} and the sensor linear range change. This is evident in Fig. 8, where the sensor output voltage as a function of the power dissipated by the heat source A is reported for two situations: in the first one, the heat source C does not dissipate any power, whereas in the second one, it dissipates a constant power of 12.48 mW, generating a temperature gradient at the temperature transducers location that superimposes to the one generated by the heat source A. Fig. 9 reports how by increasing the sensor linear range (i.e. the upper plot in Fig. 8), the sensor sensitivity has less dependence on the power dissipated by the heat source A, i.e. the sensitive is more constant along the measured dissipated power range.

3.2. *Characterization of the common mode sensitivity. DC measurements*

Ideally the output voltage of the sensor should be only sensitive to the difference of temperature between the two temperature transducers. However, like in voltage differential amplifiers, there is a common sensitivity [8]. Then, Eq. (3) becomes

$$\Delta V_{OUT} = S_{Td}(T_2-T_1)+S_{Tc}((T_2+T_1)/2) \quad (7)$$

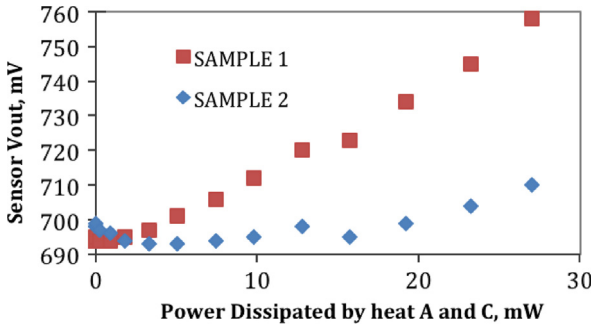

Fig. 10. Sensor output voltage as a function of the power dissipated simultaneously by heat sources A and C.

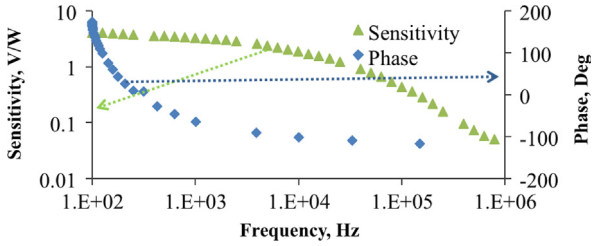

Fig. 11. Frequency response of the sensor. Sensor biased with V_{gate}= 1 V+0.05 V cos (wt). Amplitude and phase of the sensor output voltage as a function of the input frequency. Sample 1.

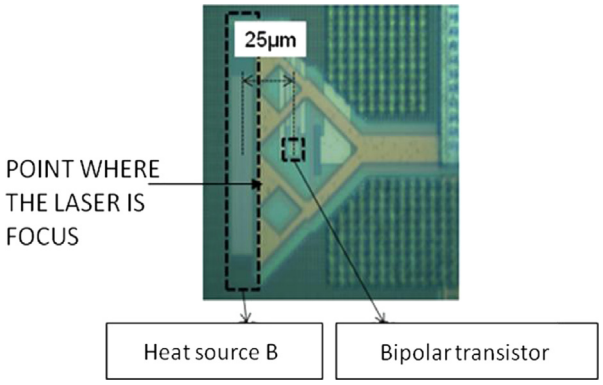

Fig. 12. Point where the laser is focused in order to perform interferometric measurements. The heat source B is a MOS transistor in diode configuration.

where S_{Tc} is the sensitivity to the common temperature (V/°C). There are two factors that make the output voltage change due to variations in the common temperature of both transducers (i.e. $(T_1+T_2)/2$). One factor is the mismatches between the two branches of the differential pair, either introduced by process variations, or introduced by the design. An example of such mismatch is the base currents that bias both temperature transducers, which are taken from one of the two branches. Another factor is the finite value of the output resistance of the current source I_{BIAS} in Fig. 3 [8].

The common mode sensitivity should be low in order to avoid output voltage changes due to ambient temperature changes or due to the power dissipated by devices that have been intentionally placed equidistant from both temperature transducers, in order to precisely cancel the sensitivity of the sensor output voltage to the power dissipated by such devices.

In order to evaluate the common mode sensitivity of the sensor, we activate simultaneously heat sources A and C with the same voltage. In this configuration they dissipate the same amount of power and, due to the placement symmetry, it is expected that they generate similar temperature increases at the transducer location. Results are shown in Fig. 10 for both measured IC samples. As it can be seen, there is variation from sample to sample: whereas in Sample 1 the output voltage changes about 60 mV when both heat sources dissipate from 0 to 28 mW of power, it only changes about 15 mV in Sample 2. In both cases, variations are almost zero for low levels of the power dissipated by the heat sources. This result reveals the impact of chip-to-chip variation on the sensor operation and stressed the importance of incorporating calibration mechanism for the sensor in case the variability observed is compromising the accuracy required for a particular application. In our experiments, the impact of the common mode sensibility can be compensate by post-measurement offset compensation, but in a practical application such offset compensation should be implemented on-chip by means of a self-calibration technique such as those routinely used in analog ICs.

3.3. *AC differential measurements*

The measurements performed in the previous sections are DC. However, in some cases (e.g. in heterodyne temperature measurements [5]) the temperature increase to be measured is sinusoidal as a function of time. The goal of this section is to extract the Bode diagram that relates the amplitude and phase of the spectral component of the sensor output voltage at the frequency f when the heat source B dissipates power following a sinusoidal function at the same frequency (i.e. the temperature increase has a sinusoidal shape as a function of time). References [8,9] show several examples of AC temperature measurements. The interest of AC measurement is to characterize the frequency response of the sensor and the frequency response of the thermal coupling between the different devices that may dissipate power and the temperature sensors. To achieve a controllable sinusoidal power dissipation, the heat source B is biased with a gate voltage V_g=1+0.05 cos ($2\pi ft$) V. With this gate voltage, the DC power dissipated by the transistor is 70 mW. Fig. 11 shows the amplitude and phase (i.e. Bode diagram) of the spectral component of the sensor output voltage at the frequency f. It is interesting to remark that this Bode diagram shows the frequency behavior of the serial connection of two transfer functions. The first one is the thermal coupling that relates the temperature increase at the transducers location as a function of the power dissipated by the transistor acting as heat source. The second one is the transfer function of the temperature sensor itself, which relates the sensor output voltage as a function of the temperature changes at the transducer location.

Looking at the results, at 100 Hz (the lowest frequency measured) the sensor has a small signal sensitivity of 4.08 V/W of magnitude and a phase shift of 173°, very close to the expected −4.1 V/W that we have measured in Fig. 6 when the DC power dissipated by the heat source was 70 mW. As the frequency increases, the sensitivity of the sensor decreases, due to the limited bandwidth of both the temperature sensor (it has a dominant pole at the output node) and the thermal coupling (all diffusion-like process have a low pass filter behavior, which can be electrically modeled with RC passive networks [8]).

With the help of a laser interferometer we have validated the AC sensor characterization. Details about the laser interferometer used as thermometer can be found in [9]. Fig. 12 indicates where the laser has been focused. Fig. 13 compares the measurements performed with the interferometer and the differential sensor, normalized to its maximum value. In this figure we have also included the analytical solution of the heat transfer equation in the Laplace domain [10]. The agreement between the three curves

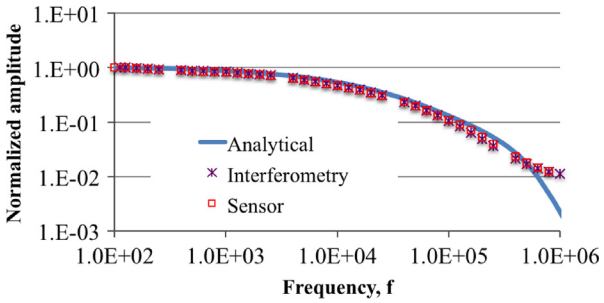

Fig. 13. Comparison of the Bode diagram amplitude obtained with the interferometer, the embedded temperature sensor and the analytical solution of the thermal coupling between the heat source B and the hot transducer. Values are normalized to its maximum value.

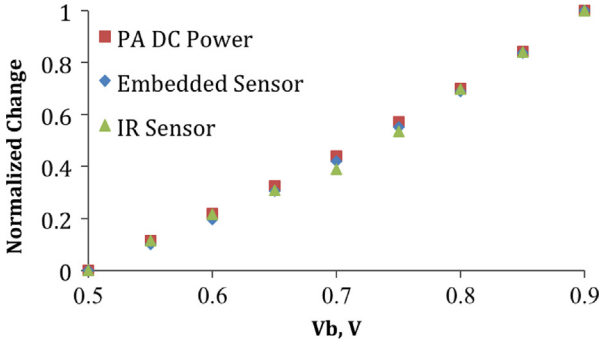

Fig. 14. Comparison of the power dissipated by the power amplifier, the embedded sensor output voltage and the IR camera readings as a function of the power amplifier bias voltage. Values are normalized to its maximum value.

indicates two important conclusions: on one hand, that the cut off frequency of this experiment is imposed by the thermal coupling limited bandwidth and not by the temperature sensor. On the other hand, the temperature sensor is measuring temperature and not an electrical coupling between the heat source and the temperature transducer.

3.4. Thermal coupling between the power amplifier and the temperature sensor

In this section we show that the temperature sensor is able to track both the DC bias and the RF activity of the PA embedded in the integrated circuit.

To illustrate that the sensor is capable to track the DC operation of the PA for various biasing conditions, we have fixed the supply voltage for the PA to 1.2 V and we have swept the V_B (see Fig. 2) from 0 V to 0.9 V. V_B controls the DC current that flows through the amplifier (B stands for BIAS) and, therefore, its DC power dissipation. The lower the V_B voltage, the lower the DC current flowing through the amplifier and the lower its DC power dissipation. Fig. 14 compares the power dissipated by the power amplifier, the information given by the embedded sensor and the IR camera. The IR measurements have been performed with a FLIR SC5500 thermal camera that employs a 320×256 InSb FPA detector. A microscopic lens [field of view (FoV) of $1.92 \times 1.53\ mm^2$] has been selected to inspect the entire surface of the IC with a spatial resolution of 6 μm. The images have been acquired at a frame rate (f_r) of 50 Hz and an integration time (t_{int}) of 1479 μs. We have focused the camera over the cascode transistor M_3 (see Fig. 1). Values in Fig. 14 are normalized to its maximum value. As it can be seen, both the readings from the IR camera and from the embedded sensor are directly proportional to the DC power dissipated by the amplifier, meaning that the embedded

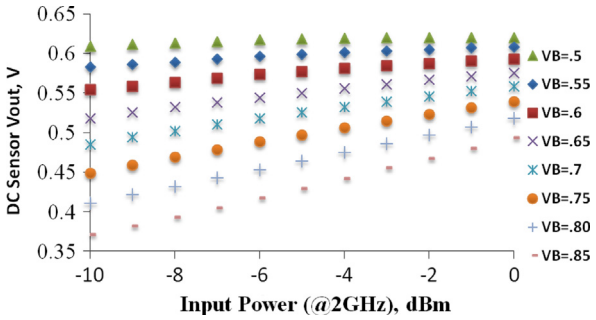

Fig. 15. Evolution of the embedded temperature sensor output voltage as a function of the PA input power for different V_B (V_{DD}=1.2 V).

temperature sensor is correctly sensing temperature increases generated by the PA DC bias.

In addition of being the sensor capable to monitor de DC bias of the PA, the RF activity of the PA can be as well monitored with temperature measurements thanks to a key property of the Joule Effect: the product of two sinusoidal electrical signals (voltage and current) of frequency f (e.g. 2 GHz) gives as result DC power dissipation (among other spectral components): it behaves like a frequency mixer. The analysis published in [11] shows that when the PA is driven with the voltage function

$$v_{in} = A\ \cos(2\pi f t) \tag{8}$$

where A is the amplitude, t is time and f is frequency; the DC power dissipated by transistors M_3 and M_1 in Fig. 2 is equal to

$$P_{DC} = V_{DD} I_{DC} - \frac{1}{2} g_m^2 A^2 R_L \tag{9}$$

where g_m is the transistor small signal transconductance of the active transistor M_1 and R_L is the passive part of the PA load at 2 GHz. Eq. (9) shows a clear relation between the DC power dissipated by the transistor and the PA gain, defined as $-g_m R_L$. The small signal transconductance of transistor M_1 (see Fig. 2) depends on the V_B value. This affects the RF gain of the PA: the lower the V_B, the lower the gain. Fig. 15 shows the dependence of the DC sensor output voltage as a function of the RF power of the signal (i.e. the amplitude A in Eqs. (8) and (9)) applied to the PA input. As expected from (9), the DC sensor depends on the amplitude of the RF signal applied to the PA input: the higher the RF input power level, the lower the temperature increase from the ambient temperature at the hot transducer location. It is interesting to see that the slope of the different plots depends on the value of V_B: the higher the slope, the higher the V_B (and, as predicted by Eq. (2), the higher the gain).

Therefore, to monitor the gain from temperature measurements, a procedure can be [6].

1. Monitoring the temperature T_1 when an RF signal with amplitude A_1 is applied to the PA input.
2. Monitoring the temperature T_2 when an RF signal with amplitude A_2 is applied to the PA input.
3. Obtaining the gain from the two temperatures, since $T_2 - T_1$ depends on the PA gain, which is an invariant in such two measurements.

4. Conclusions

In this paper we have presented design approaches and the strategy we have followed in order to characterize the thermal coupling and the performances of a differential temperature sensor implemented in a standard 65 nm CMOS technology.

We have characterized the differential and common modes operation of the embedded temperature sensor by using MOS transistors connected in diode configuration that are used as controllable heat sources. Such results indicate that the on-chip sensors are suitable for tracking the temperature changes produced by the power dissipated by devices placed in the same silicon die.

The measurements performed with the embedded temperature sensor have been corroborated with external sensing techniques: an infra-red camera and a laser interferometer used as thermometer.

Finally, we have seen that the RF performances of a PA can be tracked with DC temperature measurements.

Acknowledgments

This work has been partially supported by Feder and Spanish MICINN under the TEC2008-01856 project, by AGAUR SGR 1497 RyC2010-07434 (Ramón y Cajal contract), and TEC2011-22607 (TrenchSiC) from the Spanish Government.

References

[1] M. Pedram, S. Nazarian, Thermal modeling, analysis, and management in VLSI circuits: principles and methods, Proc. IEEE 94 (8) (2006) 1487–1501.

[2] A. Sharma, A.P. Jayasumana, Y.K. Malaiya, X-IDDQ: a novel defect detection technique using IDDQ data, in: Proceedings of the 24th IEEE VLSI Test Symposium, 2006.

[3] L. Abdallah, H.G. Stratigopoulos, S. Mir, C. Kelma, Experiences with non-intrusive sensors for RF built-in test, in: Proc. of 2012 International Test Conference, Paper 17.1, 2012.

[4] M. Onabajo, D. Gómez, E. Aldrete-Vidrio, J. Altet, D. Mateo, J. Silva-Martínez, Survey of robustness enhancement techniques for wireless systems-on-a-chip and study of temperature as observable for process variations, J. Electron. Test. 27 (3) (2011) 225–240.

[5] E. Aldrete-Vidrio, D. Mateo, J. Altet, M.A. Salhi, S. Grauby, S. Dilhaire, M. Onabajo, J. Silva-Martinez, Strategies for built-in characterization testing and performance monitoring of analog RF circuits with temperature measurements, Meas. Sci. Technol. 21 (7) (2010) 075104 (10 p.).

[6] J. Altet, D. Mateo, D. Gómez, X. Perpiñà, M. Vellvehi, X. Jordà, DC temperature measurements for the power gain monitoring in RF power amplifiers, in: Proc. of 2012 International Test Conference, Paper 17.3, 2012.

[7] C. Dufis, J.L. Gonzalez, Design of a wideband class-A power amplifier for wireline communication, in: Proc. DCIS, 2010, pp. 339–343.

[8] J. Altet, A. Rubio, E. Schaub, S. Dilahire, W Claeys, Thermal coupling in integrated circuits: application to thermal testing, IEEE J. Solid-State Circuits 36 (1) (2001) 81–91.

[9] J. Altet, S. Dilhaire, S. Volz, J.M. Rampnoux, A. Rubio, S. Grauby, L.D. Patino-Lopez, W. Claeys, J.B. Saulnier, Four different approaches for the measurement of IC surface temperature: application to thermal testing, Microelectron. J. 33 (9) (2002) 689–696.

[10] D. Millet, S. André, J.C. Barsale, A. Degiovanni, C. Moyne, Thermal Quadrupoles: Solving the Heat Equation Through Integral Transforms, Wiley, Chichester, 2000.

[11] J. Altet, D. Gómez, X. Perpinyà, D. Mateo, J.L. González, M. Vellvehi, X. Jordà, Efficiency determination of RF linear power amplifiers by steady-state temperature monitoring using built-in sensors, Sens. Actuators A Phys. 192 (2013) 49–57.